

<sup>1</sup>H. S. W. Massey and C. B. O. Mohr, Proc. Phys. Soc. (London) A67, 695 (1954). The Born term was recalculated by Cheshire (see Ref. 2), and we are in agreement with the revised calculation.

<sup>2</sup>I. M. Cheshire, Proc. Phys. Soc. (London) 83, 227 (1964).

<sup>3</sup>B. H. Bransden and Z. Jundi, Proc. Phys. Soc. (London) 92, 880 (1967).

<sup>4</sup>M. F. Fels and M. H. Mittleman, Phys. Rev. 163, 129 (1967).

<sup>5</sup>T. Roy and J. Das, Nuovo Cimento 53B, 1 (1968).

<sup>6</sup>L. Faddeev, Mathematical Aspects of the Three-Body Problem in Quantum Scattering Theory (D. Davey and Co., New York, 1965).

<sup>7</sup>R. G. Newton, Scattering Theory of Waves and Particles (McGraw-Hill Book Co., New York, 1966), p. 557.

<sup>8</sup>N. F. Mott, and H. S. W. Massey, The Theory of

Atomic Collisions, (Clarendon Press, Oxford, England, 1965), 3rd ed., p. 422.

<sup>9</sup>Positron hydrogen scattering has been extensively discussed in literature; see, for instance, W. J. Cody, J. Lawson, H. S. W. Massey, and K. Smith, Proc. Roy. Soc. (London) 278, 479 (1964). For a more recent review of all this, see P. A. Fraser in Advances in Atomic and Molecular Physics, edited by D. R. Bates and I. Estermann (Academic Press, Inc., New York, 1968), Vol. 4, p. 63.

<sup>10</sup>R. P. Feynman, Phys. Rev. 76, 769 (1949); see also J. M. Jauch and F. Rohrlich, The Theory of Photons and Electrons (Addison-Wesley Publishing Co., Inc., Reading, Mass. 1959), 2nd ed., p. 454.

<sup>11</sup>M. L. Goldberger and K. M. Watson, Collision Theory (J. Wiley & Sons, Inc., New York, 1964), p. 833.

## Phase Transitions of the Lennard-Jones System\*

Jean-Pierre Hansen and Loup Verlet

*Laboratoire de Physique Théorique et Hautes Energies, 91-Orsay, France*<sup>†</sup>

(Received 19 February 1969)

Monte Carlo computations have been performed in order to determine the phase transitions of a system of particles interacting through a Lennard-Jones potential. The fluid-solid transition has been investigated using a method recently introduced by Hoover and Ree. For the liquid-gas transition a method has been devised which forces the system to remain always homogeneous. A comparison is made with experiment in the case of argon. An indirect determination of the phase transition of the hard-sphere gas is made which is essentially in agreement with the results of the more direct calculations.

### I. INTRODUCTION

The present paper is devoted to the study of the gas-liquid and fluid-solid phase changes of a system of particles interacting through the Lennard-Jones potential

$$V(r) = 4\epsilon [(\sigma/r)^{12} - (\sigma/r)^6] . \quad (1)$$

In the one-phase region the thermodynamic properties of that system are nowadays rather well known: When the density is too high for using either the virial expansion or results from integral equations, they are obtained through Monte Carlo<sup>1-6</sup> or molecular dynamics<sup>7,8</sup> computations. These results are reviewed and discussed in Ref. 6. It has been shown furthermore<sup>1,4,8</sup> that the equilibrium properties of the system of Lennard-Jones

atoms are very similar to those of argon if  $\sigma$  and  $\epsilon$  are given those values which fit the second virial coefficient at not too low temperatures,<sup>9</sup> i. e.,  $\sigma = 3.405 \text{ \AA}$ ,  $\epsilon/k = 119.8^\circ \text{K}$ .

If one attempts "computer experiments" in the neighborhood of a phase change, one meets serious difficulties. The tendency for separation into two phases entails large fluctuations, and there is a very slow approach to "equilibrium" in the computations. It also appears difficult to reach all the relevant regions of configuration space. As a result, few quantitative results have so far been obtained.

In the liquid-gas coexistence region, Wood has studied the isotherm  $T = 1.0579$  (reduced units, i. e.,  $\sigma = \epsilon/k = 1$ , are used throughout) for a system of 32 atoms.<sup>3</sup> Owing to its small size, the system does not separate into two phases at that

temperature, and the fluctuation of the pressure should remain fairly small.

The pressure versus volume curve obtained by Wood shows a van der Waals loop in the transition region. The results are too few to allow a precise Maxwell equal area construction which would yield the transition pressure.

In the melting region, Wood and his collaborators have found in several cases that the pressure versus density curve is composed of two branches. One of these corresponds to the homogeneous solid state, the other to the pure fluid. For a 32-particle system, occasional jumps from one of these states to the other are observed in the transition region. These jumps are rare, however, so that an adequate sampling of the configuration space cannot be made. The transition pressures of the 32-particle system can therefore not be determined with any precision. For larger systems, such as the 864-particle system that we consider in the present paper, the only observed transitions are those from the fluid to the solid, and the transition pressure cannot be determined directly.

In order to locate the phase transitions we shall use methods which involve only homogeneous phases. The two-phase region with its difficulties will be completely avoided, at the price, however, of a more indirect approach.

In the condensation region, the 864-particle system exhibits large density fluctuations due to the tendency of the system to separate into regions of different densities. This problem was encountered earlier by Rotenberg<sup>10</sup> in his study of the system of 256 hard spheres each embedded in an attractive well. This author observed a van der Waals loop in the transition region, accompanied by such large fluctuations that no quantitative conclusions could be drawn. In order to avoid these difficulties, we shall devise a reversible isothermal path joining continuously the two physical one-phase states by constraining the system to remain homogeneous in the transition region. This is the spirit underlying Van Kampen's<sup>11</sup> solution of the condensation problem in the van der Waals limit. Practically, the homogeneity condition is met by subdividing the system into a certain number of boxes and, in the computer "experiments," setting upper and lower bounds to the number of atoms in each box. Large density fluctuations leading to a gradual phase separation are thus prevented and a reversible path joining the gas to the liquid phase can be constructed. The limitation in the density fluctuations is chosen so that the liquid and gas-phase thermodynamic properties are not perturbed. The pressure versus volume curve in the transition region turns out to be a van der Waals-like loop which runs smoothly into the gas and liquid isotherms. Integration of the pressure along this continuous isotherm yields the liquid-phase free energy and this in turn allows the determination of

the transition data.

In Sec. 2 of this paper, we give the results of computation, using the method that we have outlined, for two subcritical isotherms of the Lennard-Jones fluid. The calculated data are the transition pressure, densities, and latent heat. The agreement with the same quantities for argon is quite good except in the critical region, where the machine computations are unrealistic in not allowing large density fluctuations, and for the gas properties at very low temperature, where the Lennard-Jones potential is known to be inadequate.<sup>12</sup>

After the free energy of the liquid has been calculated by the above procedure, one is left with the problem of computing the free energy of the solid phase in order to determine the melting transition. A method allowing the numerical computation of the solid-phase free energy has recently been proposed by Hoover and Ree<sup>13</sup>; their method consists in stabilizing the solid phase over the whole density range by confining each atom to its own cell of volume  $V/N$  (where  $N$  is the number of atoms in the total volume  $V$ ). This scheme prevents the system from melting and provides a reversible path joining the density domain of the true solid to the low density region where the cell model free energy can be evaluated analytically. A simple integration of the pressure along an isotherm computed in this way yields the solid-state free energy. Since the free energy of the liquid is known, the transition data are easily determined.

In Sec. III, we give the results obtained using this method for the Lennard-Jones system. The thermodynamic properties of the artificial solid are computed along three different isotherms by the Monte Carlo method. These "exact" calculations have revealed a curious property of the cell model: In addition to the well-known "liquid-gas" transition of the cell model, there seems to exist a second-order phase transition at a density about 10% lower than the melting density. At very low temperatures, large fluctuations of the pressure occur and the method becomes inadequate. In that case we have solved the cell model for the Lennard-Jones potential deprived of its attractive tail, the density ranging up to that of the actual solid. The attractive part of the potential is then progressively turned on. A reversible path which makes it possible to determine the free energy of the solid is again available.

The transition data we have obtained, ranging from twice the critical temperature down to that of the triple point, are in very good agreement with those for argon. We show that along the solidification line of the Lennard-Jones fluid, the maximum of the structure factor takes the value 2.85 which is the value of the same quantity for a hard-sphere gas at solidification.

Barker and Henderson<sup>14</sup> have recently shown how a system of particles interacting through a

repulsive potential can be replaced by hard spheres. This equivalence, checked by "exact" computations, enables us to use the results of Sec. III to obtain the transition data of the hard-sphere gas. These data are very close to those obtained more directly and precisely by Hoover and Ree<sup>15</sup> who have solved the cell model for the hard-sphere system.

## II. LIQUID-GAS PHASE TRANSITION

We shall show in this section how an equation of state can be obtained for the Lennard-Jones fluid, not only for the pure one-phase states, but also in the coexistence region. Once the equation of state is known along an isotherm, the interaction part of the free energy is given by

$$\beta F_i/N = \int_0^{\rho} (\beta p/\rho' - 1) d\rho'/\rho'. \quad (2)$$

To this quantity must be added the perfect gas contribution  $\ln \rho - 1$  in order to have the total configurational part of the fluid's free energy  $F_i$  divided by  $NkT$ . From the free energy the transition densities will be obtained using the Maxwell double-tangent construction.

The equation of state in the liquid region was obtained for the reduced temperatures  $T = 1.15$  and  $T = 0.75$  by a standard Monte Carlo calculation.<sup>3</sup> A system of 864 particles with periodic boundary conditions was used. Between 3 and  $10 \times 10^5$  configurations were generated at each volume. In the course of the computation we calculated the internal energy and the compressibility factor  $\beta p/\rho$  by averaging the corresponding microscopic quantities. As the Lennard-Jones potential is cut off at  $r = 2.5 \sigma$ , a correction is made as described in Ref. 8 to take into account the effect of the neglected tail on the thermodynamical quantities. The error on  $\beta p/\rho$  is of the order of 0.02 at densities around critical and may reach 0.05 at densities around that of the triple point. The error on the internal energy is about twice smaller.

In the gas region, the equation of state can easily be obtained from the virial expansion; the densities, on the isotherms we have considered, remain sufficiently small so that using the five known virial coefficients,<sup>16</sup> we obtained a precise answer.

As we mentioned in the Introduction, the two-phase region requires more care. If we consider the 864-particle system with no constraint, it tends to separate into two phases. Owing to the rather large size of the system, this process takes a relatively long time. For instance at  $T = 1.15$  and  $\rho = 0.1$ , after  $10^6$  configurations had been generated, the pressure and internal energy had not yet reached stable values, and the computation was given up. The same result was reached for the state  $T = 0.75$ ,  $\rho = 0.05$ .

So as to obtain a faster convergence in the coexistence region, we force the system into an artificial single-phase state. In order to do so, we divide the volume into  $\nu$  cubic cells of equal size and we require the number of particles in each cell to vary only between  $\langle n \rangle - \delta n$  and  $\langle n \rangle + \delta n$ . Here  $\langle n \rangle = 864/\nu$  is the average number of particles per cell and  $\delta n$  is a fixed number. Practically this constraint is realized in the following manner: At each Monte Carlo move, we ask if the particle under consideration tries to move outside of its cell. Should it do so, the move is prevented if it violates the constraint. The constraint parameters  $\nu$  and  $\delta n$  are at our disposal. They must be chosen in such a way as to prevent the phase separation as well as possible without affecting the thermodynamical properties of the system in the physical, one-phase region.

If there is no constraint and if we are in a one-phase region, the standard deviation  $\Delta n$  to the average number of particles  $\langle n \rangle$  in a cell is given by the well-known relation

$$\Delta n = \left( 2 \langle n \rangle / \beta \frac{\partial p}{\partial \rho} \right)^{1/2}, \quad (3)$$

where  $\beta \partial p / \partial \rho$  is the inverse compressibility for the thermodynamical state under consideration. We shall choose  $\delta n$  substantially larger than  $\Delta n$  as determined in the liquid region. The constraint should therefore have no influence for the liquid. We shall check *a posteriori* that this is indeed so, and that the properties of the gas phase are not modified either.

At  $T = 1.15$ , we choose  $\nu = 27$  and  $\delta n = 12$ . For the lowest liquid density, we obtain, by numerically differentiating the computed equation of state,  $\beta \partial p / \partial \rho = 2.4$ .  $\Delta n$  is thus found to be 5.1, a value considerably smaller than  $\delta n$ . We have observed that during the computations which have actually been made in the liquid region, the constraint never operates and has therefore no measurable influence on the thermodynamics of the liquid phase.

In the gas region the constraint eliminates some possible configurations, but this has practically no influence on the equation of state. For instance for  $\rho = 0.1$ , which is a density high enough to be in the two-phase region,  $\beta p/\rho$  is equal to 0.61 when computed by the Monte Carlo method with the constraint, and to 0.613 when calculated through the virial series.

For  $T = 0.75$  the above-mentioned restriction proves insufficient; i. e., the computed thermal average fluctuates too much to allow a precise determination of the equation of state. Consequently we must take a stronger constraint. We choose  $\nu = 64$  and  $\delta n = 2.5$ . At the lowest liquid density  $\beta \partial p / \partial \rho = 12.3$ , which leads to  $\Delta n = 1.5$ . We see that  $\Delta n$  is

TABLE I. Compressibility factor and free energy per particle in the region of the liquid-gas transition for the isotherms  $T=1.15$  and  $T=0.75$ .

$\rho$	$T=0.75$		$T=1.15$	
	$\beta p/\rho$	$F_l$	$\beta p/\rho$	$F_l$
0.02	0.829	-3.81	0.918	-5.75
0.06	0.504	-3.26	0.760	-4.70
0.1	0.234	-3.08	0.612	-4.24
0.15			0.470	-3.98
0.2	-0.292	-3.07	0.345	-3.84
0.3	-0.784	-3.23	0.124	-3.74
0.4	-1.201	-3.45	-0.090	-3.74
0.5	-1.688	-3.69	-0.130	-3.77
0.55			-0.075	-3.78
0.6	-2.052	-3.93	0.070	-3.78
0.65			0.306	-3.76
0.7	-1.705	-4.15		
0.75			1.165	-3.65
0.8	-0.531	-4.27		
0.84	0.371	-4.28		
0.85			2.860	-3.38
0.92			4.723	-3.03

still somewhat smaller than  $\delta n$ . We have checked as above that the constraint, although it eliminates some configurations both in the liquid and the gas phase, has no practical effect on the thermodynamical quantities.

It should be noted that the constraint does not prevent some form of phase separation: at low densities some of the boxes tend to fill up to the maximum value,  $\langle n \rangle + \delta n$ , whereas the number of particles in other boxes decreases down to  $\langle n \rangle - \delta n$ . This separation is however rapid:  $\beta p/\rho$  reaches its equilibrium value after  $10^5$  configurations. The internal energy does not stabilize so rapidly, but this matters little as we have no use for this quantity in the two-phase region.

Table I gives the results obtained for the compressibility factor  $\beta p/\rho$  on the two isotherms  $T=1.15$  and  $T=0.75$ . The error in the two-phase region is the same as in the one-phase domain: less than 0.01 for densities less than critical, around 0.02 for densities around 0.7, somewhat more when the density is high and the temperature is low. It may reach 0.05 on the point  $\rho=0.85$ ,  $T=0.75$ . The  $\beta p/\rho$  data along an isotherm can easily be fitted by a polynomial of order 5 or 6 in  $\rho$ . Using (2) the free energy can then be obtained. The configurational part of the free energy is also given in Table I.

On Figs. 1 and 2 the pressure is represented as a function of density. It is seen that the finite system exhibits a van der Waals loop. The double-tangent construction made on the free energy ver-

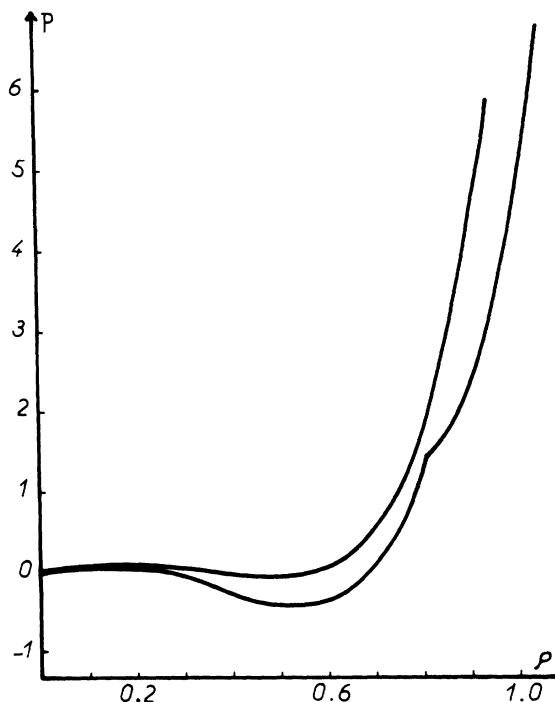


FIG. 1. Reduced pressure versus reduced density for the Lennard-Jones "homogenized" fluid (upper curve) and the corresponding cell-model (lower curve) at the reduced temperature  $T=1.15$ . Both isotherms exhibit a van der Waals loop and the cell-model isotherm exhibits an angular point around the reduced density  $\rho=0.83$ .

sus volume curve enables us to obtain the transition data. They are shown in Table II. A comparison is made with the experimental argon data.<sup>17</sup> The experimental value of the latent heat of vaporization was obtained through the Clapeyron equation.

The data of Table II together with the known critical constants for the Lennard-Jones fluid<sup>5</sup>  $T_c=1.36$ ,  $\rho_c=0.36$  are used to draw the curve shown in Fig. 3. It is seen that the coexistence curve for argon is flatter in the critical region ( $T_c=1.26$  experimentally) than the one deduced from machine computation. The long-range density variations, responsible for the peculiar singularities characteristic of the critical point, cannot be included in the Monte-Carlo calculation. If we could remove these density fluctuations in real argon, the critical temperature would probably rise to about 1.34 as shown in Ref. 6. The coexistence curve would then very much resemble that determined for the Lennard-Jones fluid.

We also notice in Table II that at very low tem-

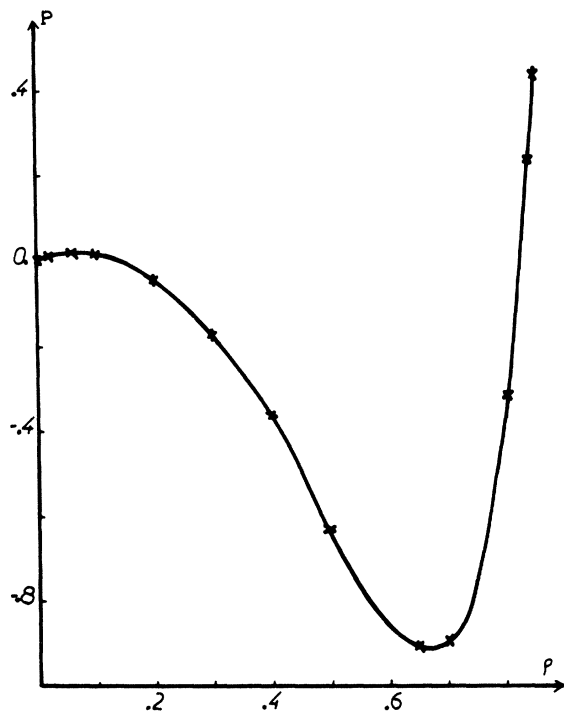


FIG. 2. Reduced pressure versus reduced density for the "homogenized" fluid at the reduced temperature  $T=0.75$ .

peratures ( $T = 0.75$ ) the transition density for the liquid branch shows a very good agreement between theory and experiment, but that there is a rather large disagreement in the case of the gas. This discrepancy is not surprising as it is well known that the properties of dilute argon at very low temperature are very poorly accounted for by the Lennard-Jones potential.<sup>12</sup> Part of the similar discrepancy for the gas at  $T = 1.15$  may also be due to the same cause. In view of the fact that the

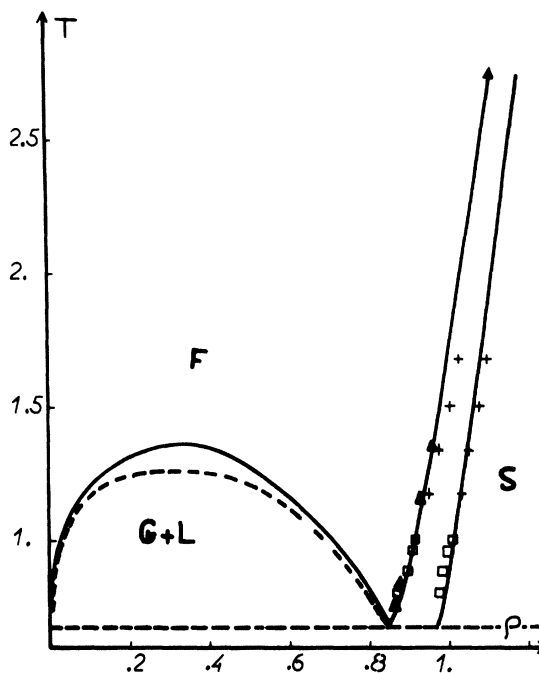


FIG. 3. Coexistence curve for the Lennard-Jones system (temperatures and densities in reduced units). The solid line gives our theoretical results. The broken line gives the experimental argon liquid-gas coexistence line taken from Michels *et al.*<sup>17,22</sup> The circles are experimental argon melting data taken from van Witenburg and Stryland,<sup>20</sup> the crosses are experimental melting data taken from Crawford and Daniels.<sup>21</sup> The triangles indicate the crystallization densities according to the "law" stating that crystallisation occurs whenever  $S(k_0)$  reaches the value 2.85.

transition pressure has been predicted quite accurately, it seems that the rather poor agreement for the latent heats is due mostly to the behavior of the low-density gas.

We have also given in Table II the results ob-

TABLE II. Liquid-gas transition data expressed in reduced units for the Lennard-Jones (LJ) fluid and for argon at the temperatures  $T = 1.15$  and  $T = 0.75$ . Here  $\mathcal{L}$  is the latent heat of melting.

		$T = 1.15$				$T = 0.75$			
		$P$	$\rho_{\text{gas}}$	$\rho_{\text{liquid}}$	$\mathcal{L}$	$P$	$\rho_{\text{gas}}$	$\rho_{\text{liquid}}$	$\mathcal{L}$
LJ	Monte Carlo	0.0597	0.073	0.606	4.34	0.0025	0.0035	0.825	6.62
	Eq. of state	0.0566	0.085	0.675	4.59	0.0034	0.0037	0.842	6.75
argon	Experiment	0.0664	0.093	0.579	3.73	0.0031	0.0047	0.818	5.44
	Eq. of state	0.0480	0.155	0.695	3.97	0.0033	0.0035	0.854	7.21

tained using the approximate equation of state of Ref. 6. We recall that these equations are supposed to hold for dense liquids and are quite poor for gases. The fit to the transition data is not very good. It is somewhat better in the Lennard-Jones case. This is probably due to the fact that the approximate equation of state for the Lennard-Jones fluid involves fewer adjustable parameters and more data with which to obtain them than is the case for argon.

### III. MELTING TRANSITION

In order to determine the melting transition, we must calculate, in addition to the free energy of the fluid which has been computed in the preceding section, that of the solid phase. The method of Hoover and Ree,<sup>13</sup> the basis of which was described in the Introduction, has been used for this purpose. It amounts to solving the cell model "exactly" for densities ranging from very small values where a suitably modified cluster expansion just ceases to apply, up to those of the actual solid. The lattice structure of the Lennard-Jones solid has been chosen to be the same as that of real argon, i. e., fcc. The corresponding cells are dodecahedra with rhombic faces.<sup>18</sup>

The numerical solution of this cell model was carried out for three isotherms:  $T=2.74$ , 1.35, and 1.15. As an example of the equation of state yielded by the model, the isotherm for  $T=1.15$  is given in Fig. 1.

The low-density behavior of the equation of state has been obtained by making a cluster expansion. If we consider a density sufficiently low so that only binary collisions occur and so that the dimension of the faces of the cells is much larger than the scale factor  $\sigma$  of the potential, the following expansion holds<sup>19</sup>:

$$\beta p/\rho = 1 + a_2' \rho^{4/3} + O(\rho^{5/3}), \quad (4)$$

$$\text{with } a_2' = -\frac{2}{3}\pi\gamma \int_0^\infty r^3 (e^{-\beta V(r)} - 1) dr, \quad (5)$$

where  $\gamma$  is a numerical factor characteristic of the cell geometry. In the case of the fcc structure, we have  $\gamma = 3 \times 2^{5/6}$ .

At higher densities, the single occupancy constraint is added to the Monte Carlo procedure used for the fluid state: Starting from a configuration where all the atoms are at the center of their cells, the atoms are moved according to the usual Metropolis procedure: The only difference is that whenever a move takes the center of an atom outside its cell the corresponding configuration is rejected. The initial configurations for which thermodynamic equilibrium has not been reached are rejected. About  $3 \cdot 10^5$  configurations are needed in order to obtain the same precision in

the pressure as was obtained for the fluid. In the computation, five shells of particles were considered around each cell. A lattice sum over the more distant shells was made in order to take the effect of the tail of the potential into account. The compressibility factor  $\beta p/\rho$  and the configurational internal energy  $U_i$  corresponding to the three temperatures  $T=2.74$ , 1.35, and 1.15 are given in Tables III, IV, and V, respectively. We also give the configurational part of the free energy  $F_S(\rho)$  obtained by integration of the equation of state over the density:

$$\beta F_S(\rho)/N = \ln \rho + \int_0^\rho (\beta p/\rho' - 1) d\rho'/\rho'. \quad (6)$$

Equation (6) differs from (2) because of the distinguishability of the particles in the cell model.

For the isotherm  $T=1.15$  we have calculated the mean-square deviation of the  $i$ th atom from the center of its cell

$$S^2 = \frac{1}{N} \sum_{i=1}^N \langle (\vec{r}_i - \vec{R}_i)^2 \rangle. \quad (7)$$

This quantity, given in Table V, is plotted as a function of the density in Fig. 4. We see that the curve consists of two very distinct branches presumably with a transition for a value of the density between 0.8 and 0.85. As may be verified in the course of the Monte Carlo computation, the low-density branch corresponds to a regime where the

TABLE III. Thermodynamic properties of the cell model for the isotherm  $T=2.74$ .

$\rho$	$\beta p/\rho$	$U_i/N$	$F_S/N$
0.05	0.949	-0.196	-8.32
0.1	0.895	-0.454	-6.57
0.2	0.803	-1.048	-4.97
0.3	0.785	-1.684	-4.09
0.4	0.851	-2.341	-3.44
0.5	1.081	-2.975	-2.86
0.6	1.486	-3.560	-2.24
0.7	2.178	-4.058	-1.49
0.8	3.21	-4.417	-0.51
0.9	4.68	-4.601	0.75
1.0	6.25	-4.77	2.32
1.05	6.99	-4.898	3.20
1.1	7.82	-4.991	4.14
1.125	8.47	-4.909	4.68
1.15	9.16	-4.816	5.18
1.2	10.65	-4.559	6.33
1.23	11.89	-4.21	7.12

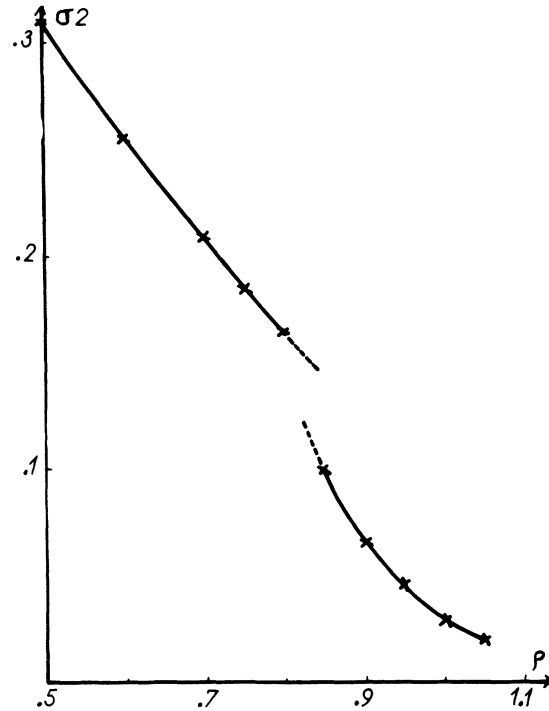
TABLE IV. Thermodynamic properties of the cell model for the isotherm  $T=1.35$ .

$\rho$	$\beta p/\rho$	$U_i/N$	$F_S/N$
0.025	0.937	-0.100	-5.03
0.05	0.851	-0.227	-4.19
0.1	0.671	-0.522	-3.47
0.15	0.477	-0.831	-3.15
0.2	0.311	-1.172	-3.00
0.25	0.140	-1.508	-2.93
0.3	0.027	-1.801	-2.91
0.35	-0.105	-2.222	-2.92
0.4	-0.186	-2.584	-2.95
0.45	-0.217	-2.943	-2.98
0.55	-0.131	-3.671	-3.03
0.6	0.07	-4.023	-3.03
0.7	0.68	-4.714	-2.97
0.8	1.79	-5.343	-2.76
0.85	2.72	-5.596	-2.57
0.9	3.34	-5.923	-2.33
0.95	3.74	-6.330	-2.07
1.	4.74	-6.611	-1.78
1.05	6.21	-6.779	-1.43
1.1	8.32	-6.78	-0.98
1.2	14.26	-6.355	0.14

localization of the particles in the cell is brought about predominantly by the cell boundaries; for the high-density branch, the localization, more pronounced (as may be seen by considering the

TABLE V. Thermodynamic properties of the cell model and mean-square deviation from the center of the cell for the isotherm  $T=1.15$ .

$\rho$	$\beta p/\rho$	$U_i/N$	$F_S/N$	$S^2$
0.05	0.820	-0.240	-3.60	
0.1	0.593	-0.538	-3.02	
0.2	0.156	-1.188	-2.72	
0.3	-0.283	-1.897	-2.75	0.48
0.4	-0.572	-2.635	-2.89	0.38
0.5	-0.678	-3.369	-3.05	0.31
0.6	-0.550	-4.110	-3.19	0.25
0.7	0.100	-4.818	-3.24	0.21
0.75	0.560	-5.162	-3.21	0.185
0.8	1.300	-5.476	-3.14	0.165
0.85	1.710	-5.865	-3.03	0.100
0.9	2.180	-6.258	-2.91	0.065
0.95	3.00	-6.592	-2.74	0.046
1.0	4.070	-6.896	-2.54	0.028
1.05	6.050	-7.015	-2.26	0.019

FIG. 4. Mean-square deviation  $s^2$  (in reduced units) of an atom from its lattice site in the cell model versus reduced density for  $T=1.15$ .

product  $S_\rho^{-1/3}$ ), is caused by the neighbors and no longer by the cells.

It is most probable that this is the explanation of what seems to be an angular point in the pressure versus density curve for the temperature 1.15. If such an angular point really exists, it means that there is, in the cell model, a second-order transition. We believe that this is indeed the case, and we give the transition densities as

$$\begin{aligned} \text{for } T=2.74, \quad \rho_t &= 1.10 \pm 0.01; \\ T=1.35, \quad \rho_t &= 0.88 \pm 0.01; \\ T=1.15, \quad \rho_t &= 0.83 \pm 0.01. \end{aligned}$$

We shall see (Table VII) that these transitions occur at densities smaller than those of the melting point. Consequently this feature of the model has no physical consequence. For densities above those transitions, the isotherms are smooth continuations of those belonging to the solids with no constraint. In Fig. 1 we see, at low density, a van der Waals loop which is also present for  $T=1.35$ . It is related to the well-known "liquid-gas" transition of the cell model.

For the temperature  $T=0.75$ , which is near the

triple point, this method is no longer feasible. At this low temperature the number of steps needed before the pressure values stabilize becomes increasingly large and this is believed to be essentially due to the attractive part of the potential. For that isotherm we used a more indirect method. As in Refs. 14 and 6 we divided the potential into two parts: The repulsive part  $u(r)$  of the Lennard-Jones potential and its attractive part  $w(r)$  multiplied by a charging parameter  $\lambda$ . The following two-step process is considered: Up to some reference density  $\rho_0 = 1.1$ , located in the physical solid phase, only the repulsive part of the interaction is taken into account, in the "exact" solution of the cell model. Using (6) we obtain the free energy  $F_S^0(\rho)$  of the system of particles interacting through  $u(r)$  when the equation of state is known on the isotherm.

The second part of the process consists of turning on the attractive potential, at the density  $\rho_0$ . We thus obtain the free energy of the solid at the density  $\rho_0$  through the easily derived relation

$$F_S(\rho_0) = F_S^0(\rho_0) + \int_0^1 \langle W \rangle_\lambda d\lambda, \quad (8)$$

where  $\langle W \rangle$  is the total attractive interaction for the interaction  $u(r) + \lambda w(r)$ , averaged over the ensemble. This quantity can be calculated by the Monte Carlo method for several values of  $\lambda$  and the integral over  $\lambda$  can be performed. The  $\lambda$  dependence of  $\langle W \rangle_\lambda$  is almost linear and it proves sufficient to perform the integral over  $\lambda$  with a step of 0.2.

Let  $\langle W \rangle_\lambda$  be expanded in powers of  $\lambda$ . The above computation shows that the contribution to the integral in (8) of the  $\lambda$ -independent term is equal to  $-7.10$ ; the term linear in  $\lambda$  yields:  $-0.38$ . The remainder of the series gives:  $0.06$ . The series seems to converge almost as well as in the case of the liquid near the triple point.<sup>6</sup>

When the free energy of the real solid is known at  $\rho_0$ , it can be calculated at neighboring values of the density by using (6), once the equation of state has been determined through the Monte Carlo method. The results of the computations made on the isotherm  $T = 0.75$  are given in Table VI. The isotherm shows, as in the case of the full Lennard-Jones potential, a branch point around  $\rho = 0.95$ .

The melting properties are given in Table VII. We give there, for the four temperatures at which the computation has been made, the melting pressures, the density of the solid at melting and that of the fluid at freezing, the volume change during the transition and the latent heat of fusion. These quantities are compared with similar quantities measured in the case of argon when they are available.<sup>20,21</sup> It is seen that the agreement is altogether surprisingly good. This confirms the excellence of the Lennard-Jones potential as an effective two-

body potential for argon at high density.

With the data of Table VII the phase diagram of Fig. 3 for the Lennard-Jones system can be completed. It is seen again that the agreement with argon data for the fluid-solid transition is quite good. From Fig. 3, the triple point can be located. It corresponds to a temperature  $T_\tau = 0.68 \pm 0.02$  and a density  $\rho_\tau = 0.85 \pm 0.01$ . These values are very near to those of argon<sup>22</sup>:  $T_\tau = 0.70$ ,  $\rho_\tau = 0.841$ .

In Fig. 5 we give the curve of melting pressure versus temperature obtained using the data of Table VII. The experimental points are shown as crosses. The triangles represent the melting results due to Barker and Henderson.<sup>23</sup> Those points are obtained through the following approximations: The liquid-state properties are given by an approximate version of the  $\lambda$  expansion,<sup>14</sup> amply discussed in Refs. 6 and 24. This theory is known<sup>14</sup> to reproduce fairly well the thermodynamical properties of the Lennard-Jones fluid. Barker and Henderson use the free-volume theory for the solid: It yields values for the free energies that are not too different from the "exact" values, as shown in Table VIII where a comparison is made for the isotherm  $T = 0.75$ . The results obtained by Barker and Henderson should lie on the curve

TABLE VI. Thermodynamic results obtained for various values of the changing parameter  $\lambda$  on the isotherm  $T = 0.75$ .

$\lambda$	$\rho$	$\beta p / \rho$	$U_i / N$	$\beta F_S / N$	$S^2$	
0	0.05	1.047	0.002	-2.96		
	0.1	1.121	0.004	-2.21	1.05	
	0.2	1.314	0.012	-1.35	0.64	
	0.3	1.652	0.024	-0.79	0.47	
	0.4	2.070	0.041	-0.25	0.38	
	0.5	2.675	0.063	0.25	0.31	
	0.6	3.46	0.092	0.81	0.265	
	0.7	4.54	0.137	1.43	0.222	
	0.8	6.01	0.195	2.12	0.190	
	0.9	8.23	0.280	2.94	0.150	
0.2	0.94	9.12	0.322	3.34	0.131	
	1.0	9.32	0.334	3.90	0.055	
	1.02	9.56	0.330	4.09		
	1.05	10.06	0.348	4.39		
	1.06	10.27	0.353	4.56	0.034	
	0	1.10	10.92	0.379	4.85	0.023
	0.2	1.10	10.42	-1.122	2.85	0.020
	0.4	1.10	9.69	-2.691	0.87	0.017
	0.6	1.10	9.36	-4.280	-1.10	0.015
	0.8	1.10	9.14	-5.903	-3.08	0.012
1.0	1.10	9.12	-7.540	-5.07	0.009	
	1.05	5.21	-7.530	-5.31	0.013	
	1.0	1.025	3.66	-7.467	-5.39	0.017
	1.0	1.0	2.35	-7.370	-5.48	0.029



TABLE VII. Fluid-solid transition data expressed in reduced units for the Lennard-Jones(LJ) fluid and for argon at the temperatures  $T=2.74, 1.35, 1.15,$  and  $0.75$ .  $\Delta V$  is the volume change at the transition.  $\mathcal{L}$  is the latent heat of melting.

	$T$	$P$	$\rho_{\text{fluid}}$	$\rho_{\text{solid}}$	$\Delta V$	$\mathcal{L}$
LJ	2.74	32.2	1.113	1.179	0.050	2.69
argon	2.74	37.4				2.34
LJ	1.35	9.00	0.964	1.053	0.087	1.88
argon	1.35	9.27	0.982	1.056	0.072	1.63
LJ	1.15	5.68	0.936	1.024	0.091	1.46
argon	1.15	6.09	0.947	1.028	0.082	1.44
LJ	0.75	0.67	0.875	0.973	0.135	1.31
argon	0.75	0.59	0.856	0.967	0.133	1.23

of Fig. 5. They are not very far off, although one should note that the pressure is plotted on a logarithmic scale.

We shall now give a relation between the crystallization of the Lennard-Jones fluid and that of a hard-sphere gas. The crystallization of a hard-sphere gas of diameter  $a$  and density  $\rho$  occurs, as we shall see in the next section, whenever the packing fraction  $\eta = \pi \rho a^3/6$  reaches the value of 0.49. Let us define the structure factor in the usual way:

$$S(k) = \sum_{i,j} \frac{\langle \exp[i\vec{k} \cdot (\vec{r}_i - \vec{r}_j)] \rangle}{N} \quad (9)$$

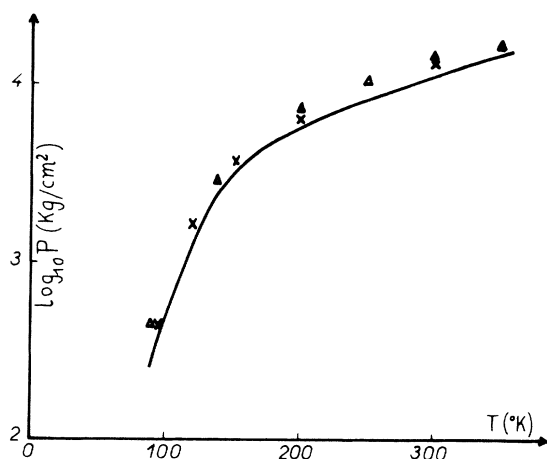


FIG. 5. Melting pressure versus temperature. The solid line gives our results for the Lennard-Jones system. The triangles are the theoretical results for the LJ system taken from Barker and Henderson<sup>23</sup>; the crosses give some experimental argon results taken from Crawford and Daniels<sup>21</sup> which are in close agreement with the results of van Witzenburg and Stryland.<sup>20</sup>

At solidification, the maximum value  $S(k_0)$  of the exactly determined<sup>25</sup> structure factor takes the value 2.85. We recall the success of a slightly modified version<sup>26</sup> of the hard-sphere model of Ashcroft and Lekner<sup>27</sup> in explaining the structure factor of the Lennard-Jones fluid: To each state of the fluid is associated a hard-sphere gas of diameter  $a(\rho, T)$  which is the only parameter of the theory. It is adjusted in such a way that  $S(k_0)$  for the hard-sphere gas of packing fraction  $\pi \rho a^3/6$  has the same value as that of the Lennard-Jones fluid at the density  $\rho$  and temperature  $T$ . The structure factor of the Lennard-Jones fluid is then very well reproduced by that of the hard-sphere gas. In view of that success it is tempting to go one step further and to associate the crystallization of the Lennard-Jones fluid with that of the underlying hard-sphere model which embodies the geometrical aspects of the problem. We then obtain a simple "law" of crystallization by stating that it should occur when  $S(k_0)$  reaches the value 2.85. In order to check this hypothesis, we need to know the structure factor for various isotherms. This can be done with the method of Ref. 26, using the correlation functions obtained in that paper and those obtained for the four isotherms studied in the

TABLE VIII. Free energy per particle in the solid phase: comparison between the prediction from free volume theory and exact results.

$\rho$	$F_i/N$	
	free volume	exact
1.01	-3.89	-4.10
1.176	-2.99	-3.07

present work.  $S(k_0)$  obtained in this way is shown for various isotherms in Fig. 6. The transition densities are obtained as intercepts of those curves with the horizontal line  $S(k_0)=2.85$ . The results are shown as triangles on Fig. 3. They are seen to agree very well with the "exact" transition curve shown on that figure. The statement that solidification occurs when the maximum value of the structure factor reaches the value 2.85 is thus confirmed.

A comparison with experiment can be made in the case of argon near its triple point. The structure factor yielded by x-ray experiments<sup>28</sup> reaches a value compatible, within the experimental errors, with the value 2.85. It would be interesting to have data relative to xenon and krypton on the solidification line.

#### IV. HARD-SPHERE TRANSITION

The calculations we have just reported for the isotherm  $T=0.75$ , where the cell model was solved exactly for a system of particles interacting through the repulsive potential  $u(r)$  can be used in order to obtain information concerning the fluid-solid transition of the hard-sphere system. The link between the two systems is provided by the work of Barker and Henderson.<sup>14</sup> These authors have shown that the system of particles interact-

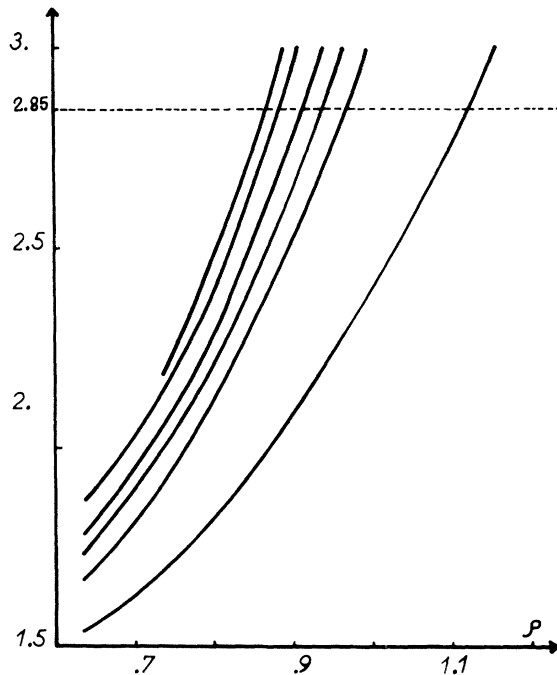


FIG. 6.  $S(k_0)$  versus reduced density along the following isotherms (in reduced units):  $T=0.75$  (upper curve), 0.833, 1., 1.15, 1.35, 2.74 (lower curve). Our empirical "law" states that crystallization takes place at the density where each of the curves intersects the horizontal line  $S(k_0)=2.85$ .

ing through  $u(r)$  at the temperature  $T$  is equivalent, as far as the thermodynamics is concerned, to a hard-sphere gas of diameter  $d$  at the same density. The diameter  $d$  is given by

$$d = \int_0^\sigma dz \{1 - \exp[-u(z)/kT]\}. \quad (10)$$

It turns out to be equal to 0.978 at  $T=0.75$ . The derivation holds both for the fluid and solid state. It is apparent that the theory is better when the density is low. It must obviously break down near the close packing of the equivalent hard-sphere system. Its range of validity can only be ascertained by direct computations. We know that for the highest densities considered in Table VI the cell model is equivalent to the real solid. We can thus compare the results with those obtained for the solid state.<sup>29,30</sup> For instance, let us consider the highest density  $\rho=1.10$ . It corresponds to a hard-sphere gas of a volume relative to that of the close packing of  $V/V_0=1.373$ . For the hard-sphere system we use the very recently published work of Alder, Hoover and Young<sup>30</sup>: By interpolating their results we obtain the value 10.9 for the compressibility factor. This should be compared with the value 10.92 of Table VI. The agreement is quite good for the other points (for  $\rho \geq 1$ ) except for the point at  $\rho=1.06$  for which the pressure is too high by about 1%.

We now are in a position to fix the tie line of the hard-sphere system: For the hard-sphere solid the free energies of Table VI are used for the density  $\rho d^3$ . The equation of state of the hard-sphere gas is well known.<sup>31,29</sup> We have a convenient fit of the exact data by adding to the known seven-term virial series<sup>32</sup> for  $p/\rho kT$  the correction<sup>6</sup>

$$1.6049 (\rho d^3)^8 + 0.46142 (\rho d^3)^{13}.$$

We find by the double-tangent construction that the melting transition occurs at  $V/V_0=1.371$  and the freezing transition at  $V/V_0=1.513$ , which corresponds to the value 0.49 for the packing fraction. Since this work was completed, Hoover and Ree have given<sup>15</sup> the solution of the cell model which was announced in their preceding paper.<sup>13</sup> They find that the tie line lies between  $V/V_0=1.359$  and  $V/V_0=1.500$ . These are very close to the figures we give. The small discrepancy is probably due to the various numerical manipulations involved in both papers.

We have made a careful comparison of the data in order to see if we can get a little more information on the transition. We have made fits for the combined data of Hoover and Ree and those of Table VI excluding only our point at  $\rho=1.06$  which is somewhat out of range. We obtain in this new revision of the data exactly the same transition data as above. It is situated between the values

1.371 and 1.513 for  $V/V_0$ .

We then obtain the thermodynamic quantities characterizing the transition similar to those found by Hoover and Ree: The communal entropy at transition is equal to 0.12; the pressure of the tie line is given by  $pV_0/NkT = 8.02$ .

### V. CONCLUSIONS

We have shown that the phase transitions of the Lennard-Jones fluid can be calculated, using methods where only homogeneous phases are con-

sidered. We plan in the near future to study the gas-solid transition at very high temperatures and to extend the same kind of methods to more complicated systems.

### VI. ACKNOWLEDGMENTS

The authors are very grateful to Dominique Levesque for his large contribution to the present work and to John Valleau for revising the manuscript.

---

\*This article is based on a thesis submitted by J. -P. Hansen for the degree of Docteur d'Etat ès Sciences Physiques at the Faculté des Sciences d'Orsay, Paris University (1969).

†Laboratoire associé au Centre National de la Recherche Scientifique.

<sup>1</sup>W. W. Wood and F. R. Parker, *J. Chem. Phys.* **27**, 720 (1957).

<sup>2</sup>W. Fickett and W. W. Wood, *Phys. Fluids* **3**, 204 (1960).

<sup>3</sup>W. W. Wood, *Physics of Simple Liquids*, edited by J. Rowlinson, G. S. Rushbrooke, and H. N. V. Temperley (North-Holland Publishing Co., Amsterdam, 1968), Chap. V.

<sup>4</sup>J. McDonald and K. Singer, *J. Chem. Phys.* **47**, 4766 (1967).

<sup>5</sup>L. Verlet and D. Levesque, *Physica* **36**, 245 (1967).

<sup>6</sup>D. Levesque and L. Verlet, *Phys. Rev.* **182**, 304 (1969).

<sup>7</sup>A. Rahman, *Phys. Rev.* **136**, A405 (1964).

<sup>8</sup>L. Verlet, *Phys. Rev.* **159**, 98 (1967).

<sup>9</sup>A. Michels, H. Wijker, and H. K. Wijker, *Physica* **15**, 627 (1949).

<sup>10</sup>A. Rotenberg, *J. Chem. Phys.* **47**, 4873 (1967).

<sup>11</sup>N. G. Van Kampen, *Phys. Rev.* **135**, A362 (1964).

<sup>12</sup>R. D. Weir, I. Wynn Jones, J. S. Rowlinson, and G. Saville, *Trans. Faraday Soc.* **63**, 1320 (1967).

<sup>13</sup>W. G. Hoover and F. H. Ree, *J. Chem. Phys.* **47**, 4873 (1967).

<sup>14</sup>J. A. Barker and D. Henderson, *J. Chem. Phys.* **47**, 4714 (1967).

<sup>15</sup>W. G. Hoover and F. H. Ree, *J. Chem. Phys.* **49**, 3609 (1968).

<sup>16</sup>J. A. Barker, P. J. Leonard, and A. Dombé, *J. Chem. Phys.* **44**, 4206 (1966).

<sup>17</sup>A. Michels, J. M. H. Levelt, and W. de Graaff, *Physica* **24**, 659 (1958).

<sup>18</sup>R. J. Buehler, R. H. Wentorf, J. O. Hirschfelder, and C. F. Curtiss, *J. Chem. Phys.* **19**, 61 (1951).

<sup>19</sup>A. Bellemans, *Physica* **28**, 493 (1962).

<sup>20</sup>W. van Witzenburg and J. C. Stryland, *Can. J. Phys.* **46**, 811 (1968).

<sup>21</sup>R. K. Crawford and W. B. Daniels, *Phys. Rev. Letters* **21**, 367 (1968).

<sup>22</sup>A. M. Clark, F. Din, J. Roob, A. Michels, A. Wasendar, and T. N. Zwietering, *Physica* **17**, 876 (1951).

<sup>23</sup>D. Henderson and J. A. Barker, *Mol. Phys.* **14**, 587 (1968).

<sup>24</sup>J. A. Barker and D. Henderson (report of work prior to publication).

<sup>25</sup>D. Schiff and L. Verlet (to be published).

<sup>26</sup>L. Verlet, *Phys. Rev.* **165**, 201 (1968).

<sup>27</sup>N. W. Ashcroft and J. Lekner, *Phys. Rev.* **145**, 83 (1966).

<sup>28</sup>N. Gingrich and C. W. Thomson, *J. Chem. Phys.* **36**, 2398 (1962).

<sup>29</sup>A. Rotenberg, New York University, Report No. NYO 1480-3, 1964 (unpublished).

<sup>30</sup>D. J. Alder, W. G. Hoover, and D. A. Young, *J. Chem. Phys.* **49**, 3688 (1968).

<sup>31</sup>B. J. Alder and T. E. Wainwright, *J. Chem. Phys.* **33**, 1439 (1968), and results quoted in Ref. 32.

<sup>32</sup>F. H. Ree and W. G. Hoover, *J. Chem. Phys.* **40**, 939 (1964).